Theoretical analysis of Lumry-Eyring models in differential scanning calorimetry

Jose M. Sanchez-Ruiz
Departamento de Quimica Fisica (Facultad de Ciencias) e Instituto de Biotecnologia, Universidad de Granada, 18071 Granada, Spain

ABSTRACT A theoretical analysis of several protein denaturation models (Lumry-Eyring models) that include a rate-limited step leading to an irreversibly denatured state of the protein (the final state) has been carried out. The differential scanning calorimetry transitions predicted for these models can be broadly classified into four groups: situations *A*, *B*, *C*, and *C'*. (*A*) The transition is calorimetrically irreversible but the rate-limited, irreversible step takes place with significant rate only at temperatures slightly above those corresponding to the transition. Equilibrium thermodynamics analysis is permissible. (*B*) The transition is distorted by the occurrence of the rate-limited step; nevertheless, it contains thermodynamic information about the reversible unfolding of the protein, which could be obtained upon the appropriate data treatment. (*C*) The heat absorption is entirely determined by the kinetics of formation of the final state and no thermodynamic information can be extracted from the calorimetric transition; the rate-determining step is the irreversible process itself. (*C'*) same as *C*, but, in this case, the rate-determining step is a previous step in the unfolding pathway. It is shown that ligand and protein concentration effects on transitions corresponding to situation *C* (strongly rate-limited transitions) are similar to those predicted by equilibrium thermodynamics for simple reversible unfolding models. It has been widely held in recent literature that experimentally observed ligand and protein concentration effects support the applicability of equilibrium thermodynamics to irreversible protein denaturation. The theoretical analysis reported here disfavors this claim.

INTRODUCTION

Equilibrium thermodynamics analysis of differential scanning calorimetry (DSC)[1] thermograms corresponding to reversible denaturation of proteins, provides detailed information about the energetics and mechanism of the reversible unfolding (Privalov, 1979, 1982, and 1989). Thus, it is possible to check the two-state character of the process and, in the case of non-two-state unfolding, to determine the number and to develop a thermodynamic characterization of the intermediate states significantly populated during unfolding (Freire and Biltonen, 1978). In addition, complex DSC thermograms can also be interpreted in terms of the more or less independent unfolding of protein domains (Privalov, 1982 and 1989); it has been recently shown (Brandts et al., 1989; Ramsay and Freire, 1990) that thermodynamic information on domain–domain interactions can be obtained from the thermograms.

The above types of analysis are based on equilibrium thermodynamics and require that the experimental heat capacity data accurately reflect the equilibrium protein unfolding (Freire and Biltonen, 1978). In principle, several factors may distort the DSC transitions and make unreliable the equilibrium thermodynamics analysis. The distortions caused by the calorimeter response time and the folding-unfolding kinetics appear to be relatively minor (at least, at moderate scanning rates), and, in any case, Lopez-Mayorga and Freire (1987) have shown how they can be corrected for. It must be recognized, nevertheless, that, in many cases, the overall process that takes place during the DSC scan is the irreversible denaturation of the protein (as shown by the lack of thermal effect in the thermogram corresponding to the second heating); in this work we will consider the distortion of the DSC transitions caused by the existence of irreversibility.

Irreversible protein denaturation is thought to involve, at least, two steps: (*a*) reversible unfolding of the native protein (N); (*b*) irreversible alteration of the unfolded protein (U) to yield a final state (F) that is unable to fold back to the native one. For a recent review on the several processes responsible for the irreversible step (aggregation, autolysis, chemical alteration of residues etc.), see Klibanov and Ahern (1987).

The two-step nature of irreversible denaturation is depicted in the following simplified scheme:

$$N \rightleftharpoons U \rightarrow F,$$

which is usually known as the Lumry and Eyring model (Lumry and Eyring, 1954). According to a point of view

[1]Abbreviations: DSC, differential scanning calorimetry; IPTG, isopropyl β-D-thiogalactoside; ONPF, *o*-nitrophenyl β-D-fucoside; Tris, tris(hydroxymethyl)aminomethane.

0006-3495/92/04/921/15 $2.00

widely held in the last 10 yr, the irreversible step (U → F) does not take place significantly during the short time the protein spends in the temperature range of the DSC transition, but occurs (with little thermal effect) at somewhat higher temperatures; it is usually assumed (see, for instance, Privalov, 1982; Privalov and Medved, 1982; Manly et al., 1985; Edge et al., 1985; Hu and Sturtevant, 1987 and 1989; Brandts et al., 1989; Bertazzon et al., 1990), therefore, that irreversible DSC transitions are due, in fact, to the reversible unfolding and are amenable to equilibrium thermodynamics analysis. Although this may be the case in some instances (see, for example, Goins and Freire, 1988), recent work has shown that, often, the irreversible step takes place, in fact, during the time the protein spends in the transition region and, therefore, the DSC transition is strongly rate limited (Sanchez-Ruiz et al., 1988a and 1988b; Guzman-Casado et al., 1990; Lepock et al., 1990; Morin et al., 1990; Freire et al., 1990; Galisteo et al., 1991; Conejero-Lara et al., 1991).

The theoretical basis of the equilibrium thermodynamics analysis of reversible DSC transitions is well established. However, theoretical studies on irreversible denaturation models (models that include rate-limited steps leading to a final state) are not available in the literature. This work is intended to fill (in part) this gap.

It must be noted that the fact that many irreversible DSC transitions are strongly rate limited has become known very recently (see the above references) and, therefore, it does not appear feasible at this time to give general recipes for the analysis of this kind of DSC transitions. The purpose of this theoretical analysis is to demonstrate (in the simplest possible manner) two important points:

(*a*) Irreversible denaturation models lead to different situations depending on the rate of the irreversible step; if this step is fast enough, the DSC transition is entirely determined by the kinetics of formation of the final state and equilibrium thermodynamics analysis is not permissible.

(*b*) Even in the case of strongly rate-limited denaturation, ligand and protein concentration effects on the DSC transitions may be observed if ligand release and protein dissociation into monomers take place before the rate-determining step; these will be shown to be nonsaturating effects, similar to those predicted by equilibrium thermodynamics for reversible unfolding transitions.

The above ideas will be demonstrated by the theoretical analysis of simple Lumry-Eyring models (see Fig. 1). Thus, point 1 will be illustrated with model II and point 2 with models IV and VI. In all cases, for the sake of simplicity, a first-order kinetics for the irreversible step (U → F) will be assumed.

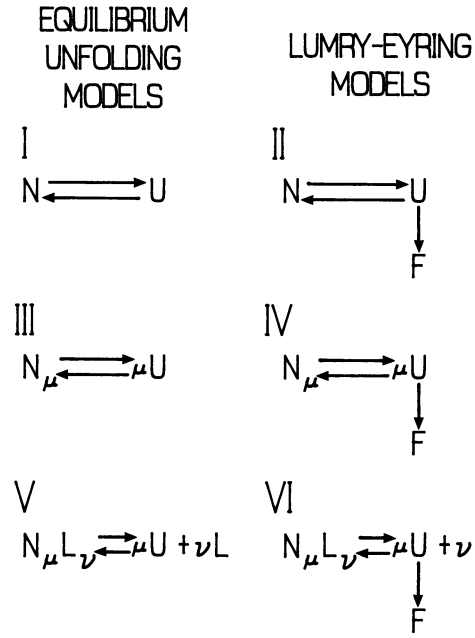

FIGURE 1 Thermal denaturation models considered in this work.

Although the models considered in this work (Fig. 1) are, in fact, very simple, we believe that the general approach employed here may enable researchers to tackle a wide variety of kinetic models. In addition, a more general scheme (which assumes that several states of the protein coexist in chemical equilibrium during denaturation and takes into account the possibility of non-first-order kinetics for the irreversible step) is briefly described in appendix 1.

THEORY AND RESULTS

The Lumry and Eyring model. The simplest form of the Lumry and Eyring model (Lumry and Eyring, 1954) can be represented by the following scheme (model II in Fig. 1):

$$N \overset{K}{\rightleftharpoons} U \overset{k}{\rightarrow} F,$$

where N, U, and F are the native, unfolded, and final (irreversibly denatured) states of the protein, respectively. We will assume that chemical equilibrium between N and U is always established and that the unfolding enthalpy, ΔH_U, is constant. Then, the temper-

ature dependence of K can be expressed as,

$$K = \frac{[U]}{[N]} = \frac{x_U}{x_N} = \exp\left\{-\frac{\Delta H_U}{R}[1/T - 1/T_{1/2}]\right\}, \quad (1)$$

where x_U and x_N stand for the molar fractions of unfolded and native states and $T_{1/2}$ is the temperature at which $K = 1$.

We will also assume that the irreversible step (U → F) is first-order and that the rate constant, k, changes with temperature according to the Arrhenius equation, which will be used in the form:

$$k(\text{min}^{-1}) = \exp\left\{-\frac{E}{R}[1/T - 1/T^*]\right\}, \quad (2)$$

where E is the activation energy and T^* is the temperature at which $k = 1$ min^{-1} [the frequency factor is equal to exp (E/RT^*)].

The rate equation for the irreversible formation of F is:

$$\frac{d[F]}{dt} = k \cdot [U], \quad (3)$$

or

$$\frac{dx_F}{dt} = k \cdot x_U, \quad (4)$$

where x_F is the molar fraction of final state. From $K = x_U/x_N$ and $x_N + x_U + x_F = 1$, it can be easily deduced that $x_U = (1 - x_F)K/(1 + K)$. Eq. 4 can, then, be rewritten as,

$$\frac{dx_F}{dt} = \frac{kK}{K+1}(1 - x_F), \quad (5)$$

which shows that, at constant temperature, x_F changes with time after a first-order kinetics with an apparent rate constant equal to $kK/(K + 1)$. In a DSC experiment, however, temperature changes with time according to a constant scanning rate ($v = dT/dt$) and the relevant differential equation is:

$$\frac{dx_F}{dT} = \frac{1}{v}\frac{kK}{K+1}(1 - x_F). \quad (6)$$

Separation of variables in Eq. 6, followed by integration from a low temperature, T_0 (at which the reaction rate is negligible and $x_F = 0$), to a temperature T, yields the temperature dependence of x_F for a DSC experiment. Then, taking into account that $K = x_U/x_N$ and $x_N + x_U + x_F = 1$, the temperature dependencies of x_N and x_U can also be obtained:

$$x_F = 1 - \exp\left\{-\frac{1}{v}\int_{T_0}^{T}\frac{kK}{K+1}dT\right\} \quad (7)$$

$$x_U = \frac{K}{K+1}\exp\left\{-\frac{1}{v}\int_{T_0}^{T}\frac{kK}{K+1}dT\right\} \quad (8)$$

$$x_N = \frac{1}{K+1}\exp\left\{-\frac{1}{v}\int_{T_0}^{T}\frac{kK}{K+1}dT\right\} \quad (9)$$

The apparent excess enthalpy, $\langle\Delta H\rangle$, is given by,

$$\langle\Delta H\rangle = x_U\Delta H_U + x_F\Delta H, \quad (10)$$

where ΔH_U and ΔH are, respectively, the enthalpies of the states U and F (taking N as the reference state). Note that the enthalpy of the final state (ΔH) is equal to the calorimetric enthalpy of the DSC transition, because eventually all protein molecules will be found in the final state.

Authors who have previously supported the applicability of the equilibrium thermodynamics analysis to irreversible DSC transitions (see, for instance, Privalov, 1982; Privalov and Medved', 1982; Manly et al., 1985) have made the (reasonable) assumption that the processes responsible for the irreversible step have much lower enthalpy than the cooperative unfolding. Clearly, if the enthalpy change for the irreversible step was large, there is no doubt that the DSC thermograms would be highly distorted. The following analysis of model II is intended to show that the DSC transitions may be distorted, even if the irreversible step has a negligible thermal effect. Accordingly, we will assume that the enthalpy of the U → F transition is zero and that, therefore, $\Delta H_U = \Delta H$. It must be noted, nevertheless, that other treatments reported in this work (ligand and protein concentration effects on irreversible DSC transitions, as well as the general scheme of Appendix 1) do not depend on this assumption.

If $\Delta H_U = \Delta H$, Eq. 10 can be written as,

$$\langle\Delta H\rangle = \Delta H\,(x_U + x_F) = \Delta H(1 - x_N), \quad (11)$$

and the apparent, excess heat capacity, C_p^{ex} is given by,

$$C_p^{ex} = -\Delta H\frac{dx_N}{dT}, \quad (12)$$

as ΔH has been assumed to be constant. Finally, dx_N/dT is obtained from Eq. 9 and substituted in Eq. 12 to yield:

$$C_p^{ex} = \frac{K\Delta H}{(K+1)^2}\left\{\frac{k}{v} + \frac{\Delta H}{RT^2}\right\}\exp\left\{-\frac{1}{v}\int_{T_0}^{T}\frac{kK}{K+1}dT\right\}. \quad (13)$$

It is interesting that the equation corresponding to a two-state reversible unfolding (model I in Fig. 1):

$$C_p^{ex} = \frac{\Delta H^2}{RT^2}\frac{K}{(K+1)^2} \quad (14)$$

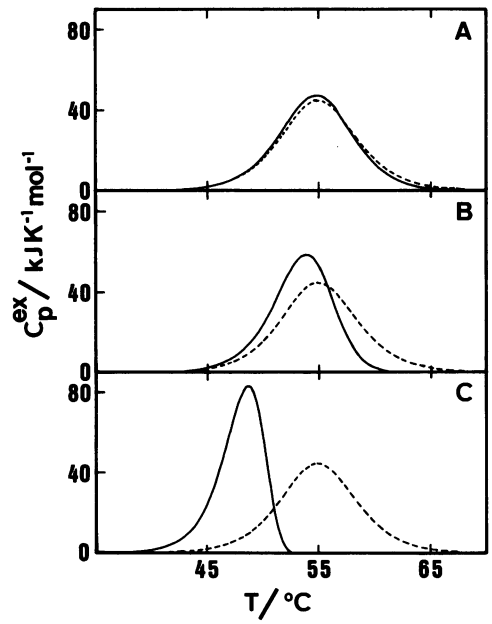

FIGURE 2 DSC transitions predicted by Eq. 13 (model II) and the following parameters: ΔH = 400 kJ/mol; $T_{1/2}$ = 55°C; E = 100 kJ/mol; v = 2 K/min. (*A*) T^* = 75°C; (*B*) T^* = 55°C; (*C*) T^* = 25°C. In all cases, the dashed transition corresponds to the reversible unfolding (Eq. 14).

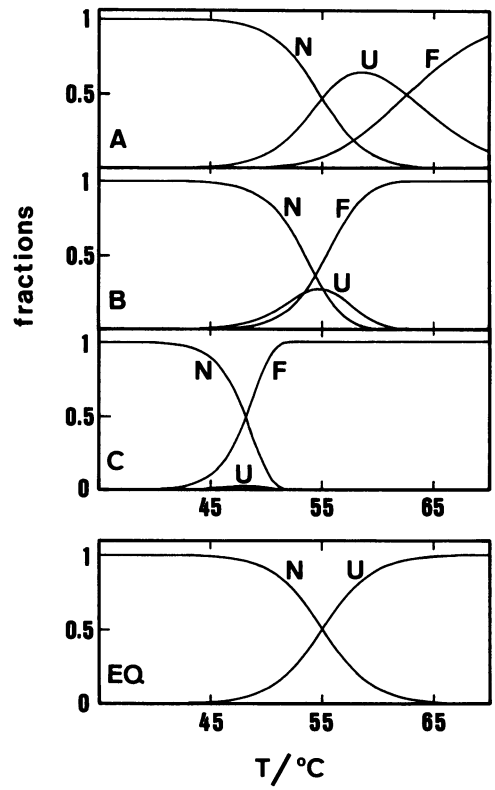

FIGURE 3 (*A*, *B*, and *C*) Fraction of states *versus* temperature profiles corresponding to the DSC transitions of Fig. 2 (model II). The profiles were calculated by using Eqs. 7, 8, and 9 and the parameters given in the legend of Fig. 2. (*EQ*) Fraction of states *versus* temperature profile corresponding to the reversible equilibrium unfolding.

can be derived from Eq. 13 either by setting $k = 0$ at any temperature (the irreversible process does not take place) or by setting $1/v = 0$ (infinite scanning rate).

The DSC transitions predicted by Eq. 13 can be broadly classified into three groups, that will be referred to as situations A, B, and C. These are illustrated by the traces shown in Fig. 2, which correspond to the same values of ΔH (400 kJ/mol), $T_{1/2}$ (55°C), E (100 kJ/mol), and v (2 K/min), and different values of T^* (the corresponding population of states *versus* temperature profiles are given in Fig. 3). The values chosen for ΔH and $T_{1/2}$ are within the ranges found for small globular proteins (Privalov, 1979), while the one for the energy of activation, E, is close to that determined by Goins and Freire (1988) for the irreversible step in the thermal denaturation of the B subunit of cholera toxin.[2]

Situation A (Figs. 2 A and 3 A). In this case T^* = 75°C, the irreversible step proceeds at significant rate only at temperatures above $T_{1/2}$ (55°C) and, in fact, the calorimetric trace differs little from that corresponding to the reversible unfolding (model I in Fig. 1). At $T = T_{1/2}$, x_F is very low; however, at T = 70°C (a few degrees above the end of the transition), most of the protein is in the final state, F (Fig. 3*A*). Therefore, if the DSC scan is terminated at 70°C, no significant heat effect will be

[2]Recent DSC studies on the irreversible thermal denaturation of several proteins (Sanchez-Ruiz et al., 1988a and 1988b; Guzman-Casado et al., 1990, Lepock et al., 1990; Morin et al., 1990; Conejero-Lara et al., 1991) report energies of activation within the range ~150–~600 kJ/mol. In these studies, however, the DSC transitions were found to conform to two-state irreversible models and, therefore, they correspond to what we call situations C/C'; the theoretical analysis reported in this work shows that, in these situations, the energy of activation is an apparent value (E_{app}), which is not equal to the energy of activation for the irreversible step (E). On the other hand, Goins and Freire (1988) have shown that the irreversible step in the thermal denaturation of the B subunit of cholera toxin takes place (with negligible thermal effect) at temperatures somewhat above than those corresponding to the DSC transition (this case is referred to in this work as situation A); therefore, they were able to study the irreversible step separately and the energy of activation reported by these authors (~100 kJ/mol) does correspond to the irreversible step itself. In this work, E = 100 kJ/mol is employed as demonstration value for the simulations of model II; it must be noted, nevertheless, that situations A, B, and C are also obtained with values for E much lower (and much higher) than 100 kJ/mol. In fact, the specific values of the parameters (ΔH, $T_{1/2}$, and E, for model II) are not critical for the general result of the simulation. This remark also applies to all other simulations described in this work.

observed in the reheating run and the transition will be considered as calorimetrically irreversible. In spite of that, it is clear that direct application of equilibrium thermodynamics to the irreversible transition in Fig. 2 *A* would not lead to large errors.

Situation B (Figs. 2B and 3B). Here, $T^* = 55°C$ and the irreversible step is fast in the temperature range of the reversible unfolding. The DSC transition deviates clearly from that corresponding to the equilibrium unfolding (Fig. 2 *B*) and direct application of equilibrium thermodynamics would lead to significant errors. There exist, however, a significant amount of unfolded state in equilibrium with the native one during the temperature-induced denaturation (Fig. 3 *B*); that is, the calorimetric transition contains thermodynamic information about the reversible unfolding, which could be obtained upon the appropriate data treatment (see Appendix 1).

Situation C (Figs. 2 C and 3 C). In this case, $T^* = 25°C$, the irreversible step being fast at temperatures well below $T_{1/2}$ (55°C). The T_m value (temperature corresponding to the maximum heat capacity) is several degrees lower than the one for the reversible unfolding (Fig. 2 *C*) and only the states N and F are significantly populated (Fig. 3 *C*). Thus, the irreversible transition in Fig. 2 *C* can be described by the so-called two-state irreversible model (Sanchez-Ruiz et al., 1988a):

$$N \xrightarrow{kK} F,$$

where the apparent first-order rate constant for the process is equal to kK, given that, within the temperature range of this transition, $K \ll 1$ and $K + 1 \simeq 1$ (see Eq. 5). Equilibrium thermodynamic analysis of this transition would lead to gross errors. In addition, the small amount of U, together with the experimental uncertainties (noise, baseline tracing, etc.) found in a real DSC experiment, would preclude the determination of any thermodynamic information about the reversible unfolding step.

The three situations (A, B, and C) have been simulated in Figs. 2 and 3 by using different values of the parameter T^*. These situations, however, can also be achieved (Fig. 4) by changing the scanning rate while keeping constant ΔH, $T_{1/2}$, and T^*. For the transitions of Fig. 4, $\Delta H = 400$ kJ/mol, $T_{1/2} = 55°C$, $T^* = 55°C$, and the scanning rate has been changed from 10^2 K/min to 10^{-4} K/min. The transition corresponding to the highest scanning rate does not differ significantly from that for the reversible unfolding, while those obtained within the scanning rate range 10^{-2}–10^{-4} K/min correspond to situation C and are described by the two-state irreversible model. (The transitions of Fig. 4 are shown for illustration purposes: it must be noted that the total scanning rate range employed is much wider than the one usually available to the experimenter; in addition, it does not appear likely that chemical equilibrium between the native and unfolded states of the protein be established at the higher scanning rates.)

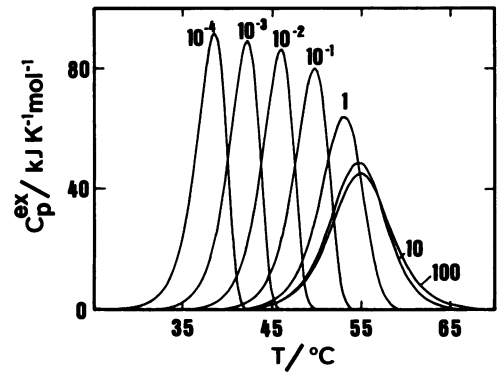

FIGURE 4 Scanning rate effect on DSC transitions corresponding to model II. These transitions have been calculated by using Eq. 13 and the following parameters: $\Delta H = 400$ kJ/mol; $T_{1/2} = 55°C$; $E = 100$ kJ/mol; $T^* = 55°C$. The numbers alongside the transitions stand for the scanning rate in K/min.

The DSC transitions in Figs. 2 and 4 have been calculated assuming that the rate-limiting step is the irreversible process (U → F) itself, and that chemical equilibrium between the states N and U is always established. A more general treatment of model II (Fig. 1) would require that the kinetics of the unfolding–refolding processes be taken into account, according to the following scheme:

$$N \underset{k_2}{\overset{k_1}{\rightleftharpoons}} U \xrightarrow{k} F,$$

where we will assume that all the kinetic processes are first-order and the unfolding equilibrium constant is given by $K = k_1/k_2$. In this scheme the rate-limiting step is determined by the relative values of the rate constants k and k_2 (Jencks, 1987; Lowry and Richardson, 1976).

If $k_2 \gg k$, most of the U molecules will be able to refold to the native state, as a result the equilibrium between N and U will be established and the calorimetric transitions will be described by Eq. 13. If, in addition, $K \ll 1$, the amount of U will be very low and the rate of formation of F will be determined by an apparent first-order rate constant equal to kK (Jencks, 1987); this is, in fact, the situation C described above.

If $k \gg k_2$, most of the U molecules will be converted to the final state, F, instead of refolding to the native state through the process U → N, the concentration of U will be very low and chemical equilibrium between U and N will not be established. In this case, the rate-

limiting step is the unfolding (N → U) and the formation of F is determined by a first-order rate constant equal to k_1 (Jencks, 1987; see, also, Sanchez-Ruiz et al., 1988a):

$$N \xrightarrow{k_1} F.$$

This case will be referred to as Situation C'. At least for model II with first order kinetics, both situations, C and C', are described by the two-state irreversible model and cannot be distinguished on the basis of the DSC transitions, the only difference being the rate-determining step.

Concentration effects on DSC transitions corresponding to irreversible protein denaturation. Equilibrium thermodynamics predicts that, for the simple equilibrium model (model III in Fig. 1):

$$N_\mu \overset{K}{\rightleftharpoons} \mu U,$$

in which a multimeric protein undergoes two-state reversible unfolding with simultaneous dissociation into monomers, the temperature of the maximum of the DSC transitions, T_m, increases with the total protein concentration according to (Takahashi and Sturtevant, 1981):

$$\Delta H^{vH}/RT_m + (\mu - 1) \ln C_t = \text{constant}, \qquad (15)$$

where ΔH^{vH} is the so-called van't Hoff enthalpy[3] and C_t is the total protein concentration. It must be noted that the ΔH^{vH} value can be independently calculated from the shape of the transitions according to the well known equation:

$$\Delta H^{vH} = ART_m^2 C_{p,m}^{ex}/\Delta H, \qquad (16)$$

where $C_{p,m}^{ex}$ and ΔH are the excess heat capacity at the maximum and the denaturation enthalpy (values of the constant A for several values of μ are given by Manly et al., 1985; see also Table 1).

The Lumry and Eyring model corresponding to model III is:

$$N_\mu \overset{K}{\rightleftharpoons} \mu\, U \underset{F}{\downarrow k},$$

which is model IV in Fig. 1. Depending on the rate of the irreversible step, this model will lead to different situations; here, however, we will be interested in situation C. Therefore, we will assume that the equilibrium between the native and the unfolded states is always established (the temperature dependence of the unfolding equilibrium constant being described by Eq. 1) and that the amount of unfolded state is always very low. It will also be assumed that the irreversible step is determined by a first-order rate constant that changes with temperature according to the Arrhenius equation (Eq. 2).

The rate of formation of the final state is given by Eq. 3 ($d[F]/dt = k[U]$), which can also be written as:

$$\frac{dC_F}{dt} = kC_U, \qquad (17)$$

where C_F and C_U stand for the concentrations in mg/ml, and the unfolding equilibrium constant is defined as:

$$K = \frac{[U]^\mu}{[N_\mu]} = \mu M^{(1-\mu)} \frac{C_U^\mu}{C_N}, \qquad (18)$$

where [U] and $[N_\mu]$ are the concentrations in mol/liter, C_U and C_N are the concentrations in mg/ml, and M stands for the monomer molecular weight. Eq. 17 and 18 can be combined to yield:

$$\frac{dC_F}{dt} = k_{app} C_N^{1/\mu}, \qquad (19)$$

where k_{app} is an apparent rate constant given by:

$$k_{app} = k \left(\frac{K}{\mu}\right)^{1/\mu} M^{(\mu-1)/\mu}. \qquad (20)$$

Given that k_{app} is proportional to $kK^{1/\mu}$, and that both, k

TABLE 1 Apparent van't Hoff enthalpies that would be obtained by applying equilibrium thermodynamics to rate-limited DSC transitions corresponding to models IV and VI in situation C

μ	A*	$\mu^{1/(\mu-1)}$	$\Delta H^{vH‡}$	$\Delta H^{vH§}$	$\Delta H^{vH‖}$
1	4.00	2.72¶	1.47 E_{app}	—	E_{app} 32%
2	5.83	2.00	2.92 E_{app}	2 E_{app} 31.5%	2 E_{app} 31.5%
3	7.43	1.73	4.29 E_{app}	3 E_{app} 30%	3 E_{app} 30%
4	9.01	1.59	5.67 E_{app}	4 E_{app} 29.5%	4 E_{app} 29.5%

*Coefficient A in Eq. 16; taken from Manly et al. (1985).
‡Calculated from the shape of the transitions according to Eq. 16.
§Calculated from the protein concentration effect on the T_m values, according to Eq. 15; the percentages refer to the deviations from the values obtained by using Eq. 16.
‖Calculated from the ligand effect on the T_m values, according to Eq. 29; the percentages refer to the deviations from the values obtained by using Eq. 16.
¶$\lim_{\mu\to 1} \mu^{1/(\mu-1)} = e = 2.718\ldots$

[3]Eqs. 15 and 29 are valid for two-state reversible unfolding models (models III and V in Fig. 1); therefore, the van't Hoff enthalpy, ΔH^{vH}, should equal the true or calorimetric enthalpy, ΔH. These equations, however, have often been used for non-two-state reversible unfolding cases ($\Delta H^{vH} \neq \Delta H$).

and K, are assumed to show exponential dependence with $1/T$, it is clear that the temperature dependence of k_{app} can be expressed by an Arrhenius equation:

$$k_{app} = \exp\left(-\frac{E + \Delta H_U/\mu}{R}\left(\frac{1}{T} - \frac{1}{T^*}\right)\right)$$
$$= \exp(E_{app}/RT^*)\exp(-E_{app}/RT)$$
$$E_{app} = E + (\Delta H_U/\mu), \quad (21)$$

where T^* is the temperature at which $k_{app} = 1$ (in units of min^{-1} $(mg/ml)^{(\mu-1)/\mu}$), E is the energy of activation of the irreversible step (U → F), and ΔH_U is the unfolding enthalpy. Note, however, that the temperature dependence of k_{app} is determined by the value of $E + \Delta H_U/\mu$; that is, $E + \Delta H_U/\mu$ plays the role of an apparent energy of activation: E_{app}.

For situation C, the total protein concentration can be expressed as $C_t \simeq C_N + C_F$. Accordingly, $dC_N/dt = -dC_F/dt$ and Eq. 19 becomes:

$$\frac{dC_N}{dt} = -k_{app}C_N^{1/\mu}, \quad (22)$$

and for a DSC experiment the relevant differential equation is:

$$\frac{dC_N}{dT} = -(1/v)\,k_{app}(T)C_N^{1/\mu}, \quad (23)$$

where v is the scanning rate (dT/dt) and $k_{app}(T)$ is the temperature-dependent value of k_{app} given by Eq. 21.

DSC traces corresponding to model IV in situation C were calculated by using the following procedure: Eq. 23 was integrated numerically (using the fourth-order Runge-Kutta algorithm with an integration interval of 0.02°C) from a low temperature T_0 (at which the rate is negligible and $C_N = C_t$) to a temperature T. This integration leads to the temperature dependence of C_N and dC_N/dT (Eq. 23). Finally, the excess heat capacity was obtained according to,

$$C_p^{ex} = -\Delta H\frac{d(C_N/C_t)}{dT} = -(\Delta H/C_t)\frac{dC_N}{dT}, \quad (24)$$

as the denaturation enthalpy, ΔH, is assumed to be constant. These C_p^{ex}/T profiles depend on the values chosen for the following parameters: μ, v, C_t, ΔH, T^*, and E_{app}. In the simulations described below $E_{app} = 300$ kJ/mol is always employed (see footnote 2); of course, this value may be obtained from different sets of ΔH_U and E values (for instance, for $\mu = 2$, it is obtained from $\Delta H_U = 400$ kJ/mol and $E = 100$ kJ/mol, or from $\Delta H_U = 500$ kJ/mol and $E = 50$ kJ/mol, or . . .); note, however, that the DSC transitions do not depend on the values of ΔH_U and E, but only on $(E + \Delta H_U/\mu)$, which is the apparent energy of activation: E_{app} (see Eq. 21).

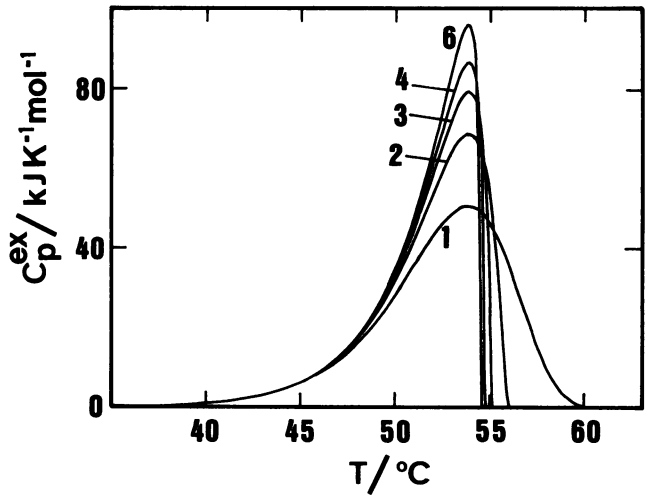

FIGURE 5 Effect of the value of μ on the asymmetry of DSC transitions corresponding to model IV in situation C. These transitions have been calculated by numerical integration of Eq. 23 (see text) with the following parameters: $\Delta H = 400$ kJ/mol; $E_{app} = 300$ kJ/mol; $T^* = 55$°C; $v = 2$ K/min; $C_t = 1$ mg/ml. The numbers alongside the transitions stand for the values of μ.

Fig. 5 shows several simulated DSC transitions in which the parameters ΔH (400 kJ/mol), E_{app} (300 kJ/mol), T^* (55°C), v (2 K/min), and C_t (1 mg/ml) have been kept fixed and the value of μ has been changed from $\mu = 1$ to 6. In all cases, the transitions are asymmetrical, the asymmetry being more pronounced for the higher values of μ.

Except for $\mu = 1$ (which corresponds, in fact, to model II), the DSC transitions for model IV in situation C depend strongly on the total protein concentration. This is evident in Fig. 6 *A*, which shows the effect of C_t (0.5–20 mg/ml) for DSC transitions characterized by $\Delta H = 400$ kJ/mol, $E_{app} = 300$ kJ/mol, $T^* = 55$°C, $v = 2$ K/min, and $\mu = 4$.

Mathematical elaboration of model IV in situation C (Appendix 2) leads to several useful relationships that give:

(*a*) the scanning rate effect on T_m (at constant C_t):

$$\ln(v/T_m^2) = \text{constant} - \frac{E_{app}}{RT_m}; \quad (25)$$

(*b*) the shape of the transitions:

$$C_p^{ex} = \frac{\Delta H E_{app}}{RT_m^2}\exp\left(\frac{E_{app}\Delta T}{RT_m^2}\right) \times\left(1 + \frac{1-\mu}{\mu}\exp\left(\frac{E_{app}\Delta T}{RT_m^2}\right)\right)^{1/(\mu-1)}, \quad (26)$$

where $\Delta T = T - T_m$;

(*c*) the apparent energy of activation in terms of the parameters corresponding to the maximum of the transition:

$$E_{app} = \mu^{1/(\mu-1)} RT_m^2 C_{p,m}^{ex} / \Delta H; \quad (27)$$

(*d*) the effect of the total protein concentration on the temperature corresponding to the maximum heat capacity (at constant scanning rate):

$$\frac{E_{app}}{RT_m} - 2 \ln T_m + \frac{\mu - 1}{\mu} \ln C_t = cte. \quad (28)$$

For reasonable values of E_{app}, the term $2 \ln T_m$ changes with T_m much more slowly than does the term E_{app}/RT_m; hence, the term $2 \ln T_m$ can be taken as a constant and, therefore, Eq. 28 predicts that a plot of $\ln C_t$ *versus* $1/T_m$ should be linear with a slope equal to $-\mu E_{app}/(\mu - 1)R)$. The T_m values for the transitions of Fig. 6*A*, in fact, fit quantitatively this prediction (see Fig. 6*B*). It must be noted that the protein concentration effects predicted by the equilibrium unfolding model III (Eq. 15) and the Lumry-Eyring model IV in situation C (Eq. 28) are similar; thus, in both cases the effect is nonsaturating and plots of $\ln C_t$ *versus* $1/T_m$ are linear.

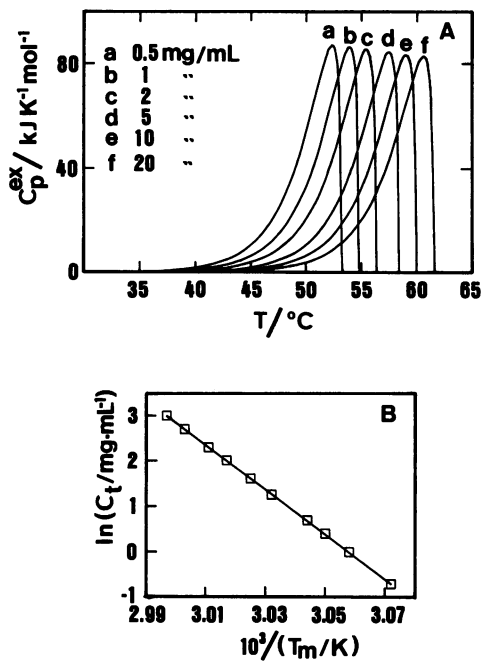

FIGURE 6 Protein concentration effect on DSC transitions corresponding to model IV in situation C. (*A*) DSC transitions calculated by numerical integration of Eq. 23 (see text) with the following parameters: ΔH = 400 kJ/mol; E_{app} = 300 kJ/mol; T^* = 55°C; μ = 4; v = 2 *K*/min. The numbers alongside the transitions stand for the total protein concentrations (C_t) in mg/ml. (*B*) Plot of $\ln C_t$ versus $1/T_m$ for the transitions in Fig. 5*A* (additional T_m values [corresponding to 1.5, 3.5, 7.5, and 15 mg/ml] are included); the straight line has the slope $(-\mu E_{app}/[R(\mu - 1)])$ predicted by Eq. 28.

Ligand effects on DSC transitions corresponding to irreversible protein denaturation. Equilibrium thermodynamics predicts that, for the equilibrium model (model V in Fig. 1):

$$N_\mu L_\nu \overset{K}{\rightleftharpoons} \nu L + \mu U,$$

in which the protein undergoes two-state unfolding with simultaneous dissociation and ligand loss, the effect of ligand and total protein concentrations on the temperature of the maximum of the DSC transitions is given by (Fukada et al., 1983):[3]

$$\frac{\Delta H^{vH}}{RT_m} + \nu \ln L_0 + (\mu - 1) \ln C_t = \text{constant}, \quad (29)$$

where L_0 is the ligand concentration (Eq. 29 corresponds to the case in which the concentration of ligand is much larger than that of protein).

The Lumry and Eyring model corresponding to model V is

$$N_\mu L_\nu \overset{K}{\rightleftharpoons} \nu L + \mu \underset{\downarrow k}{U}$$
$$F$$

which is model VI in Fig. 1.

The unfolding equilibrium constant, *K*, is defined by:

$$K = \frac{[U]^\mu [L]^\nu}{[N_\mu L_\nu]} = \mu M^{(1-\mu)} 10^{-3\nu} \left(\frac{C_U^\mu L_0^\nu}{C_N} \right), \quad (30)$$

where *M* is the monomer molecular weight, [U], [L], and $[N_\mu L_\nu]$ are the concentrations in mol/liter, C_U and C_N are the concentrations in mg/ml, and L_0 is the ligand concentration in mM (it is convenient to use these units, as they correspond to the usual protein and ligand concentration ranges employed in DSC studies).

In this case, the rate of formation of the final state is also given by Eq. (17) and, following the same procedure employed with model IV, it is straightforward to arrive to:

$$\frac{dC_N}{dt} = -k_{app} L_0^{-\nu/\mu} C_N^{1/\mu}, \quad (31)$$

where the apparent rate constant is given by:

$$k_{app} = k \left(\frac{K}{\mu} \right)^{1/\mu} M^{(\mu-1)/\mu} 10^{3\nu/\mu}. \quad (32)$$

The assumptions made in deriving Eq. 31 are the same as in model IV. In addition, we have assumed that the ligand concentration is much larger than the total

protein concentration and, therefore, the former can be taken as a constant in a given DSC experiment. It is also important to note that Eq. 31 is valid exclusively for situation C (the concentration of U is very low and only the states $N_\mu L_\nu$ and F are significantly populated).

As was the case for model IV, k_{app} is proportional to $kK^{1/\mu}$ and, therefore, its temperature dependence can be described by Eq. 21 with an apparent energy of activation, E_{app}, and a temperature, T^*, at which $k_{app} = 1$ (in units of min^{-1} $(mg/ml)^{(\mu-1)/\mu}$ $mM^{\nu/\mu}$). Thus, for a DSC experiment,

$$\frac{dC_N}{dT} = -(1/v)\, k_{app}(T) L_0^{-\nu/\mu} C_N^{1/\mu}, \qquad (33)$$

where $k_{app}(T)$ is the temperature dependent value of k_{app} given by Eq. 21. Eq. 33 can be written as,

$$\frac{dC_N}{dT} = -(1/v)\, k'_{app}(T, L_0) C_N^{1/\mu}, \qquad (34)$$

where $k'_{app} = k_{app} L_0^{-\nu/\mu}$. For a given DSC experiment, however, L_0 is constant and Eq. (34) is equivalent to Eq. (23). Therefore, Eqs. 25 (scanning rate effect), 26 (shape of the transitions), and 27 (energy of activation in terms of the parameters of the maximum) hold true for model VI in situation C (see Appendix 2).

Of course, in this case there is ligand concentration effect on the transitions. This effect (together with the total protein concentration effect) is given by (Appendix 2):

$$\frac{E_{app}}{RT_m} - 2 \ln T_m + \frac{\mu - 1}{\mu} \ln C_t + \frac{\nu}{\mu} \ln L_0 = \text{constant}. \qquad (35)$$

Thus, the effect of C_t on T_m (at constant L_0 and scanning rate) is the same as that described for model IV in situation C (Eq. 28). In addition, the T_m value increases with the ligand concentration (at constant C_t and scanning rate) and a plot of $\ln L_0$ versus $1/T_m$ will be linear with a slope equal to $-\mu E_{app}/(\nu R)$ (given that the term $2 \ln T_m$ can, in fact, be taken as a constant).

Fig. 7 *A* shows the effect of the ligand concentration (0.5–20 mM) on DSC transitions characterized by the following parameters: $\Delta H = 400$ kJ/mol, $E_{app} = 300$ kJ/mol, $T^* = 55°C$, $\mu = 4$, $\nu = 4$, $C_t = 1$ mg/ml, and $v = 2\,K/min$. These transitions were calculated by numerical integration of Eq. 33 (as described for model IV). The effect of L_0 on T_m is quantitatively described by Eq. 35 (Fig. 7 *B*). Therefore, we find that, both, the equilibrium unfolding model V (Eq. 29 and the Lumry-Eyring model VI (Eq. 35 predict a nonsaturating ligand effect and that plots of $\ln L_0$ versus $1/T_m$ are linear.

It is worth noting here that, in models IV and VI (Fig. 1), the equilibrium unfolding step leads to the unfolded monomer (U), which, subsequently, undergoes the irreversible process to give the final state. We could have devised similar models in which the first step led, for instance, to folded monomers (N). This, however, would not make any difference for situation C, in which the amount of monomeric species is very low. Thus, the conclusions reached in our treatment of models IV and VI in situation C (Eqs. 25, 26, 27, 28, and 35) remain valid if we assume that the unfolding step leads to, in general, an intermediate monomeric species (folded, unfolded, or partially folded).

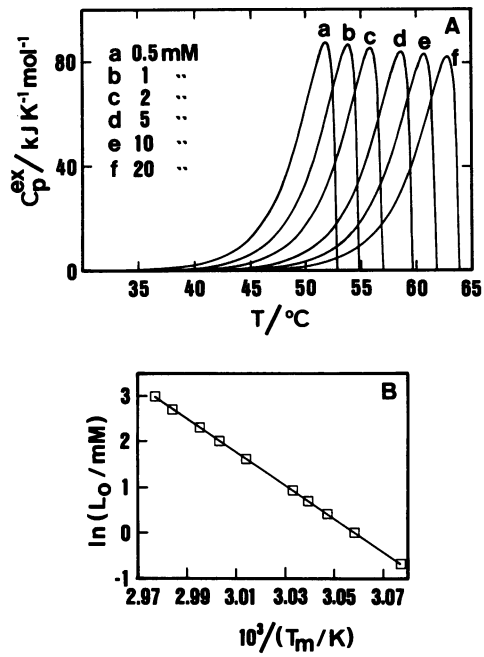

FIGURE 7 Ligand concentration effect on DSC transitions corresponding to model VI in situation C. (*A*) DSC transitions calculated by numerical integration of Eq. 33 (see text) with the following parameters: $\Delta H = 400$ kJ/mol; $E_{app} = 300$ kJ/mol; $T^* = 55°C$; $\mu = 4$; $\nu = 4$; $v = 2\,K/min$; $C_t = 1$ mg/ml. The numbers alongside the transitions stand for the ligand concentrations (L_0) in mM. (*B*) Plot of $\ln L_0$ versus $1/T_m$ for the DSC transitions in Fig. 6*A* (additional T_m values [corresponding to 1.5, 2.5, 7.5, and 15 mM] are included); the straight line has the slope $(-\mu E_{app}/(\nu R))$ predicted by Eq. 35.

DISCUSSION

Lumry and Eyring models lead to different situations depending on the rate of the irreversible process. In two of these situations (C and C', the difference being the rate determining step) chemical equilibrium between the significant populated states is not established and the relative amounts of these states during denaturation are given by the integration of a rate equation (not by a temperature-dependent equilibrium constant). Situa-

tions C/C′ are not just theoretical possibilities; in fact, they correspond to the so-called two-state irreversible model, which has been recently demonstrated for the thermal denaturation of several proteins (Sanchez-Ruiz et al., 1988a and 1988b; Guzman-Casado et al, 1990; Lepock et al., 1990; Morin et al., 1990; Conejero-Lara et al., 1991).

Equilibrium thermodynamics analysis of DSC transitions in situation C/C′ is not permissible. This statement means that: (*a*) the denaturation entropy change (and, hence, the denaturation Gibbs energy change) cannot be determined from the transitions, given that entropy calculations from experimental heat capacity data are based upon the Clausius equality, which does not hold for an irreversible, rate-limited process; (*b*) analysis of the transition shapes based on the assumption that two or more protein states coexist in equilibrium during the scan are obviously incorrect. (It must be noted, nevertheless, that, according to the first law, the total heat absorbed equals the denaturation enthalpy change, even if the denaturation process is irreversible. Of course, this denaturation enthalpy will be the enthalpy difference between the final and native states.)

The main experimental evidence supporting equilibrium thermodynamics analysis of irreversible DSC transitions comes from the fact that, in several cases (see Manly et al., 1985; Edge et al., 1985; Hu and Sturtevant, 1987), ligand and protein concentration effects on the transitions conform to Eqs. 15 and 29, which are derived from equilibrium unfolding models (models III and V in Fig. 1); that is, plots of ln C_t and ln L_0 versus $1/T_m$ are often found to be linear (within the scatter of the experimental data), and the ΔH^{vH} values obtained from the slope of these plots show a "rough" agreement with those calculated from the shape of the transitions (Eq. 16).

The analysis of models IV and VI reported here shows, however, that the T_m values may increase with ligand and protein concentrations and that plots of ln L_0 and ln C_t versus $1/T_m$ may be linear, even in cases of strongly rate-limited denaturation. In addition, it is not at all clear whether a "rough" agreement between the ΔH^{vH} values derived from the plots of ln L_0 and ln C_t versus $1/T_m$ and those calculated from Eq. 16 proves conclusively that the denaturation follows equilibrium thermodynamics. For instance (see Table 1), if Eq. 16 is applied to a DSC transition corresponding to models IV or VI in situation C, the apparent ΔH^{vH} value obtained would, in fact, be equal to $AE_{app}/\mu^{1/(\mu-1)}$ (compare Eqs. 16 and 27); the values derived from the ligand and protein concentration effects (compare Eqs. 29 and 35) would be equal to μE_{app}. In Table 1 we show the apparent ΔH^{vH} values that would be obtained for several values of μ (1–4); the percentage deviation between the ΔH^{vH} values is ~30%; that is, there is a rough agreement. It must be noted that the Lumry-Eyring models we have analyzed (as well as the reversible unfolding models: I, III, and V) are very simple ones; even if a good agreement between the several ΔH^{vH} values is experimentally found, the possibility that more complex kinetic models could also explain the data must be considered.

It appears, therefore, that ligand and protein concentration effects are not reliable equilibrium criteria in DSC of proteins. This statement can be illustrated with a specific example; Manly et al. (1985) carried out a DSC study on the irreversible thermal denaturation of the tetrameric (μ = 4) core protein of *lac* repressor in phosphate buffer 0.048 M, pH 7.4, 15% glycerol, 0.1 mM dithiothreitol. They found that, in the absence of ligands, the shape of the DSC transitions and the total protein concentration effect on the T_m values could be interpreted on the basis of the reversible unfolding model III with μ = 4. However, the shape of the transitions can also be explained by model IV in situation C, as shown in Fig. 8 *A*; in addition, the plot of T_m *versus* C_t of Fig. 8 *B*, in which the data reported by Manly et al. are compared with the theoretical curve predicted by Eq. 28 with the E_{app} value (372 kJ/mol) calculated from the shape of the transitions (Eq. 27), shows that the observed protein concentration effect is also consistent with model IV in situation C. Manly et al. also found an effect of the ligands IPTG and ONPF on the DSC transitions, which was explained (qualitatively) on the basis of the equilibrium model V with ν = 4; thus, plots of ln L_0 *versus* $1/T_m$ were linear, but the ΔH^{vH} values derived from the slopes (3,025 kJ/mol for IPTG and 4489 kJ/mol for ONPF) were in poor agreement with those calculated from the shape of the transitions by using Eq. 16 (1766 kJ/mol for IPTG and 1715 kJ/mol for ONPF). If the plots of ln L_0 *versus* $1/T_m$ are interpreted according to Eq. 35 (model VI in situation C), values of E_{app} = 756 kJ/mol for IPTG and E_{app} = 1122 kJ/mol for ONPF are obtained. Again, these values are in very poor agreement with the ones calculated from the shape of transitions (Eq. 27): E_{app} = 311 kJ/mol for IPTG and E_{app} = 303 kJ/mol for ONPF. It appears, therefore, that neither model V nor model VI in situation C are able to account (in a quantitative manner) for the observed ligand effects. Of course, both models can be "improved"; for instance, Manly et al. pointed out that the discrepancy between the ΔH^{vH} values could be removed if only three or less molecules of ligand were bound to the native protein at denaturational temperatures ($\nu \leq 3$). Obviously, this procedure would also work for model VI in situation C.

The fact that the ligand and protein concentration effects for models VI and IV in situation C are similar to those predicted by equilibrium unfolding models was to

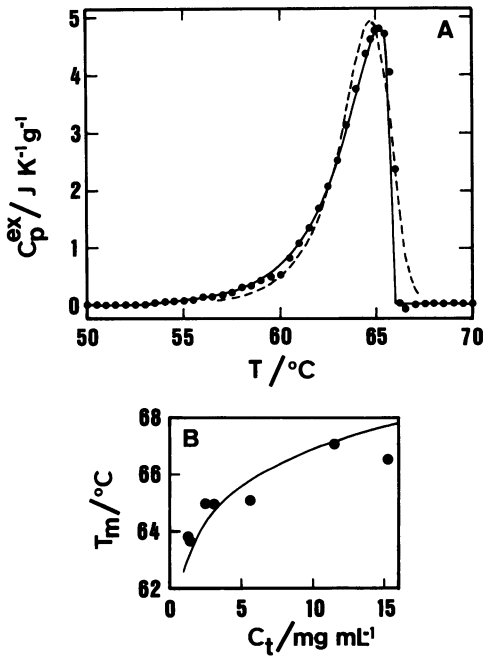

FIGURE 8 (*A*) DSC thermogram for the irreversible thermal denaturation of the core protein of *lac* repressor (pH = 7.4; C_t = 5.74 mg/ml; v = 0.23 *K*/min). (●) Experimental data, taken from Manly et al. (1985). (---) Best fit of the theoretical curve for model III with μ = 4, taken from Manly et al. (1985). (——) Best fit of the theoretical curve for model IV in situation C (Eq. 26) with μ = 4. (*B*) protein concentration effect on the T_m values for the thermal denaturation of the core protein. (●) Experimental data, taken from Manly et al. (1985). (——) Curve predicted by Eq. 28 (model IV in situation C) with μ = 4 and the E_{app} value (372 kJ/mol) derived from the shape of the transitions according to Eq. 27.

be expected: in situation C the rate limiting step is the irreversible process itself (U → F), the concentration of unfolded state (or intermediate state, in general) is very low, but chemical equilibrium between the native and unfolded (or intermediate) states is established (this kind of kinetic mechanism is sometimes referred to as "preliminary equilibrium mechanism"; see Lowry and Richardson, 1976). Clearly, any factor that "displaces" the preliminary equilibrium will affect the rate of formation of the final state; thus, increasing the total protein concentration (models IV and VI) or the ligand concentration (model VI) originates a lower molar fraction of unfolded (or intermediate) state, a lower rate of formation of the final state (per mole of protein) and a shift of the DSC transitions to higher temperatures. Accordingly, we believe that our conclusions can be stated in a general way.

(*a*) For a strongly rate-limited, irreversible DSC transition, protein concentration effects may be expected to occur if the dissociation of the native multimeric protein into monomers takes place before the rate-determining step (even if no dissociation takes place before the rate-determining step, protein concentration effects may occur if the kinetics of the irreversible process is not first order; see Galisteo et al. [1991]).

(*b*) For a strongly rate-limited, irreversible DSC transition, ligand concentration effects may be expected to occur if ligand dissociation takes place before the rate-determining step.

In general, these effects are not expected to be much different than those predicted by equilibrium unfolding models, given that their origin is the preliminary equilibrium step.

Finally, it is interesting to note that recent DSC studies on irreversible protein denaturation have yielded results that appear difficult to rationalize on the basis of equilibrium thermodynamics. Thus, it has been found in some cases (Edge et al., 1985; Guzman-Casado et al., 1990) that the T_m values corresponding to the irreversible denaturation of multimeric proteins do not change with protein concentration; according to equilibrium thermodynamics, this means that the unfolded protein remains in the same oligomerization state as the native one (Edge et al., 1985), which appears to suggest that the specific monomer–monomer interactions responsible for the multimeric character of the native protein are still present in the unfolded state. It has also been reported (Edge et al., 1985; Hu and Sturtevant, 1989) that, in some cases, increasing the ligand concentration causes irreversible DSC transitions to shift to lower temperatures; this result has been explained, in terms of equilibrium thermodynamics, by assuming that the ligand binds more tightly to the unfolded protein than to the native one (Edge et al., 1985; Hu and Sturtevant, 1989), which appears to suggest that the binding site for the ligand is still formed in the unfolded protein.

The results described above, however, can be easily understood if one assumes that the irreversible DSC transitions are strongly rate limited. Thus, a lack of protein concentration effect on the T_m values for the denaturation of multimeric proteins is to be expected if protein dissociation into monomers does not take place before the rate-determining step and the irreversible process shows first-order kinetics. In addition, a lowering of the T_m values upon increasing ligand concentration could simply mean that the ligand increases the rate of irreversible denaturation (if, for instance, both the native protein with (NL) and without (N) bound ligand can react irreversibly to yield the final state (F), being the rate of the process NL → F + L faster than that of the process N → F). Of course, these kinetic explanations make no assumption regarding the oligomerization state or the ligand-binding characteristics of the unfolded protein.

CONCLUDING REMARKS

It has been widely held in the literature that irreversible alterations of the unfolded state do not distort significantly the DSC transitions, but take place at somewhat higher temperatures; this is equivalent to assume that protein thermal stability is determined by equilibrium factors (the unfolding Gibbs energy *versus* temperature profile), even when denaturation is overall irreversible. The fact that, in some cases, ligand and protein concentration effects on irreversible DSC transitions appear to conform to the dictates of equilibrium thermodynamics has been claimed to support the above point of view. However, the theoretical analysis reported in this work highly disfavors this claim; in addition, recent experimental studies have shown that, often, irreversible DSC transitions are strongly rate limited. It appears very likely, therefore, that, in many cases of irreversible denaturation, operational thermal stability (as measured by the denaturation temperature under given conditions) is subject to kinetic constraints. This fact ought to have influence, not only on DSC data analysis, but also on the approaches employed to obtain modified proteins with enhanced thermal stability; thus, equilibrium approaches (such as introducing mutations that are thought to increase the unfolding Gibbs energy) might not be adequate in some cases of irreversible denaturation, while changes (in the protein or in the solvent conditions) that decrease the rate of irreversible denaturation might be found to be more successful.

APPENDIX 1

Multistate denaturation mechanism including irreversibility

Assume that several, significantly populated states of the protein (I_0, I_1, I_2, I_3 ... I_n) coexist in chemical equilibrium during the thermally-induced denaturation and that any (or, in general, all) of the I_i states undergo an irreversible, rate-controlled conversion to a final state F. The concentrations of states are related by:

$$C_{eq} = \sum_i C_i \quad C_t = C_{eq} + C_F, \tag{A1.1}$$

where C_t is the total protein concentration, C_F is the concentration of final state, C_i is the concentration of a state I_i, and C_{eq} the total concentration of states I_i in equilibrium. The fractions of states are given by,

$$x_i = C_i/C_t = \frac{C_i}{C_{eq} + C_F} \quad x_F = C_F/C_t = \frac{C_F}{C_{eq} + C_F}, \tag{A1.2}$$

where x_i and x_F are, respectively, the fractions of states I_i and F. We define a second set of fractions (y_i), only for those states in equilibrium:

$$y_i = C_i/C_{eq}. \tag{A1.3}$$

The two sets of fractions are related by,

$$y_i = \frac{x_i}{1 - x_F}. \tag{A1.4}$$

The apparent excess enthalpy, $\langle \Delta H \rangle$, is an average over all the protein states:

$$\langle \Delta H \rangle = x_F \, \Delta H + \sum_i x_i \, \Delta H_i, \tag{A1.5}$$

where ΔH_i is the enthalpy difference between the state I_i and the reference state I_0 (i.e., the native state). Note that the enthalpy difference between the state F and the state I_0 is equal to the total enthalpy change of the transition, ΔH, as eventually all the protein molecules will be found in the state F.

Again, we define another excess enthalpy, $\langle \Delta H \rangle_e$, for the states I_i exclusively:

$$\langle \Delta H \rangle_e = \sum_i y_i \, \Delta H_i. \tag{A1.6}$$

The relationship between both excess enthalpies can be easily derived by combining Eqs. A1.4–6:

$$\langle \Delta H \rangle = (1 - x_F) \langle \Delta H \rangle_e + x_F \, \Delta H. \tag{A1.7}$$

$\langle \Delta H \rangle$ *versus* temperature profiles can be obtained from the experimental excess heat capacity data by integration. However, the thermodynamic information associated with the DSC transitions is contained in the $\langle \Delta H \rangle_e/T$ profile (note that $\langle \Delta H \rangle_e$ is an average over the states I_i in equilibrium only). If the $\langle \Delta H \rangle_e/T$ profile can be extracted from the experimental data, then it can be analyzed using the equilibrium thermodynamic procedure.

Assume that the rate of formation of the final state is given by[4]:

$$-\frac{d C_F}{dt} = \frac{d C_{eq}}{dt} = -k_{app} C_{eq}^n, \tag{A1.8}$$

or for a DSC experiment at constant scanning rate (v),

$$\frac{d C_{eq}}{dT} = -(1/v) \, k_{app} C_{eq}^n, \tag{A1.9}$$

where n is the reaction order and k_{app} is an apparent n-order rate constant. k_{app} may, in general, be a complicated expression including individual rate constants (corresponding to irreversible steps: $I_i \rightarrow F$) and equilibrium constants (corresponding to reversible steps: $I_i \leftrightarrow I_{i+1}$); it is assumed, however, to depend only on temperature. For instance, in model II only two states of the protein coexist in equilibrium (I_0 = N and I_1 = U), the reaction order is unity and the apparent rate constant is given by $k_{app} = kK/(K + 1)$ (Eq. 5).

Separation of variables in Eq. A1.9 followed by integration from a low temperature, T_0, at which the reaction rate is negligible and

[4]Eq. A1.8 assumes that the collection of states I_i in equilibrium behaves as a single species from the kinetic point of view, as is to be expected on general grounds.

essentially all the protein is in the native state, leads to:

$$C_{eq}^{(1-n)} - C_t^{(1-n)} = \frac{(n-1)}{v} F(T), \qquad \text{(A1.10)}$$

where $F(T)$ is the following integral:

$$F(T) = \int_{T_0}^{T} k_{app}\, dT. \qquad \text{(A1.11)}$$

From Eq. A1.10 the following can be easily obtained,

$$x_F = 1 - \left(1 + \frac{(n-1)}{v} C_t^{(n-1)} F(T)\right)^{1/(1-n)}, \qquad \text{(A1.12)}$$

which, substituted in Eq. A1.7, yields:

$$\Delta H - \langle \Delta H \rangle = (\Delta H - \langle \Delta H \rangle_e) \times \left(1 + \frac{(n-1)}{v} C_t^{(n-1)} F(T)\right)^{1/(1-n)}, \qquad \text{(A1.13)}$$

or

$$(\Delta H - \langle \Delta H \rangle)^{1-n} = (\Delta H - \langle \Delta H \rangle_e)^{1-n} + \frac{(n-1)}{v} (\Delta H - \langle \Delta H \rangle_e)^{1-n} C_t^{(n-1)} F(T). \qquad \text{(A1.14)}$$

Thus, at constant T and C_t, a plot of $(\Delta H - \langle \Delta H \rangle)^{1-n}$ *versus* $1/v$ should result in a straight line; $\langle \Delta H \rangle_e$ and $F(T)$ could then be obtained from the intercept and slope of that line (of course, a nonlinear least squares analysis based on Eq. (A1.13) would also be possible). This procedure should be applied to several temperatures (within the denaturational range) to produce the $\langle \Delta H \rangle_e / T$ profile (thermodynamic information associated with the DSC transitions) and the $F(T)/T$ profile (kinetic information about the irreversible formation of F). Note that, if this procedure is applied to DSC transitions in situation C, $\langle \Delta H \rangle_e$ values close to zero will be obtained, indicating that no information about the equilibrium unfolding is associated with the transitions.

Eq. A1.13 is valid for $n \neq 1$. The equation corresponding to $n = 1$ can be easily shown to be:

$$(\Delta H - \langle \Delta H \rangle) = (\Delta H - \langle \Delta H \rangle_e)\, e^{-F(T)/v}. \qquad \text{(A1.15)}$$

APPENDIX 2

Transitions shape and effects of ligand concentration, protein concentration, and scanning rate for models IV and VI in situation C

We will carry out the derivations specifically for model VI (model IV can be considered a particular case of model VI for the case in which $\nu = 0$). The differential equation corresponding to a DSC experiment (Eq. 33 in the text) is:

$$\frac{dC_N}{dT} = -\frac{1}{v} k_{app} L_0^{-\nu/\mu} C_N^{1/\mu}, \qquad \text{(A2.1)}$$

where k_{app} depends on temperature according to,

$$k_{app} = \exp(E_{app}/RT^*) \exp(-E_{app}/RT), \qquad \text{(A2.2)}$$

which is Eq. 21 in the text. Note that, for a given DSC experiment, the scanning rate (v) and the ligand concentration (L_0) are taken as constants.

Condition of the maximum of the DSC transitions. For $T = T_m$ we have that $dC_p^{ex}/dT = 0$ and, therefore, $(d^2C_N/dT^2)_m = 0$. Applying this condition to Eq. A2.1 we obtain:

$$0 = \left(\frac{dk_{app}}{dT}\right)_m C_{N,m}^{1/\mu} + k_{app,m} \frac{1}{\mu} C_{N,m}^{(1-\mu)/\mu} \left(\frac{dC_N}{dT}\right)_m, \qquad \text{(A2.3)}$$

or

$$(d \ln k_{app}/dT)_m = -\frac{1}{\mu} (d \ln C_N/dT)_m, \qquad \text{(A2.4)}$$

where $C_{N,m}$, $k_{app,m}$, $(d \ln k_{app}/dT)_m$, *and* $(d \ln C_N/dT)_m$ are the values of C_N, k_{app}, $(d \ln k_{app}/dT)$, and $(d \ln C_N/dT)$ at $T = T_m$. Finally, taking into account Eqs. A2.1 and A2.2, the following is easily arrived at,

$$\mu \frac{E_{app}}{R} \exp(-E_{app}/RT^*) = \frac{T_m^2}{v} \exp(-E_{app}/RT_m) L_0^{-\nu/\mu} C_{N,m}^{(1-\mu)/\mu}. \qquad \text{(A2.5)}$$

Temperature dependence of the concentration of native protein. Separation of variables in Eq. A2.1, followed by integration from a temperature, T_0, low enough to make the reaction rate negligible, leads to:

$$C_N^{(\mu-1)/\mu} = C_t^{(\mu-1)/\mu} + \frac{(1-\mu)}{\mu v} L_0^{-\nu/\mu} F(T), \qquad \text{(A2.6)}$$

where C_t is the total protein concentration (for $T = T_0$, $C_N = C_t$) and $F(T)$ is the following integral:

$$F(T) = \int_{T_0}^{T} k_{app}\, dT = \exp(E_{app}/RT^*) \int_{T_0}^{T} \exp(-E_{app}/RT)\, dT. \qquad \text{(A2.7)}$$

Eq. A2.6 can also be written as:

$$x_N = \left(1 + \frac{(1-\mu)}{\mu v} L_0^{-\nu/\mu} C_t^{(1-\mu)/\mu} F(T)\right)^{\mu/(\mu-1)}, \qquad \text{(A2.8)}$$

where x_N ($= C_N/C_t$) is the fraction of protein that remains in the native state at the temperature T.

The integral in Eq. (A2.7) does not have an exact closed form solution. An approximate expression for $F(T)$, valid within the relatively narrow temperature range of a DSC transition, can be obtained, however, by taking into account that, within that temperature range, $1/T$ can be approximated by (Sanchez-Ruiz et al., 1988a):

$$1/T = 1/T_m - \Delta T/T_m^2, \qquad \text{(A2.9)}$$

where $\Delta T = T - T_m$. Substituting A2.9 into A2.7 and integrating from

ΔT_0 ($\Delta T_0 = T_0 - T_m$) to ΔT, we arrive at,

$$F(T) = \frac{1}{W}\exp\left\{\frac{E_{app}}{R}\left(\frac{1}{T^*} - \frac{1}{T_m}\right)\right\} \{\exp(W\Delta T) - \exp(W\Delta T_0)\}, \quad \text{(A2.10)}$$

where $W = E_{app}/RT_m^2$. If T_0 is low enough, and for the temperature range of the calorimetric transition, $\exp(W\Delta T_0) \ll \exp(W\Delta T)$. Therefore, and taking into account Eq. A2.5, $F(T)$ can be expressed as:

$$F(T) = \mu\upsilon L_0^{\nu/\mu} C_{N,m}^{(\mu-1)/\mu} \exp(E_{app}\Delta T/RT_m^2). \quad \text{(A2.11)}$$

Substituting Eq. A2.11 into A2.8, we obtain,

$$x_N = (1 + (1 - \mu) x_{N,m}^{(\mu-1)/\mu} \exp(E_{app}\Delta T/RT_m^2))^{\mu/(\mu-1)}, \quad \text{(A2.12)}$$

where $x_{N,m}$ ($= C_{N,m}/C_t$) is the fraction of protein that remains in the native state at the temperature T_m. For $T = T_m$, $\Delta T = 0$ and $x_N = x_{N,m}$; therefore.

$$x_{N,m} = (1 + (1 - \mu) x_{N,m}^{(\mu-1)/\mu})^{\mu/(\mu-1)}, \quad \text{(A2.13)}$$

from whence,

$$x_{N,m} = \mu^{\mu/(1-\mu)}. \quad \text{(A2.14)}$$

Finally, substituting Eq. A2.14 into A2.12 the following is arrived at:

$$x_N = \frac{C_N}{C_t} = \left(1 + \frac{(1 - \mu)}{\mu}\exp(E_{app}\Delta T/RT_m^2)\right)^{\mu/(\mu-1)}, \quad \text{(A2.15)}$$

which gives the temperature dependence of the concentration of native protein.

Scanning rate, ligand concentration, and protein concentration effects on the DSC transitions. Substituting Eq. A2.14 into A2.5 yields:

$$\frac{E_{app}}{R}\exp(-E_{app}/RT^*) = \frac{T_m^2}{\upsilon}\exp(-E_{app}/RT_m) L_0^{-\nu/\mu} C_t^{(1-\mu)/\mu}. \quad \text{(A2.16)}$$

Therefore, at constant L_0 and C_t, the scanning rate effect on the DSC transitions is described by,

$$\ln(\upsilon/T_m^2) = \text{constant} - \frac{E_{app}}{RT_m}, \quad \text{(A2.17)}$$

and, at constant scanning rate, the ligand and protein concentration effects on the transitions are given by:

$$\text{constant} = \frac{E_{app}}{RT_m} - 2\ln T_m + \frac{(\mu - 1)}{\mu}\ln C_t + \frac{\nu}{\mu}\ln L_0. \quad \text{(A2.18)}$$

Temperature dependence of the apparent excess heat capacity. The apparent excess heat capacity if given by,

$$C_p^{ex} = -(\Delta H/C_t)\frac{d C_N}{dT} = -\Delta H\frac{dx_N}{dT}, \quad \text{(A2.19)}$$

dx_N/dT can be obtained from Eq. A2.15 and substituted into Eq. A2.19 to yield[5],

$$C_p^{ex} = \frac{\Delta H E_{app}}{RT_m^2}\exp\left(\frac{E_{app}\Delta T}{RT_m^2}\right) \times \left\{1 + \frac{(1 - \mu)}{\mu}\exp\left(\frac{E_{app}\Delta T}{RT_m^2}\right)\right\}^{1/(\mu-1)}. \quad \text{(A2.20)}$$

Taking the $\mu \to 1$ limit in Eq. A2.20 the following is obtained:

$$C_p^{ex} = \frac{\Delta H E_{app}}{RT_m^2}\exp\left(\frac{E_{app}\Delta T}{RT_m^2}\right) \times \exp\left\{-\exp\left(\frac{E_{app}\Delta T}{RT_m^2}\right)\right\}, \quad \text{(A2.21)}$$

which corresponds to $\mu = 1$, that is, to the two-state irreversible model with first-order kinetics (Sanchez-Ruiz et al., 1988a).

Setting $T = T_m$ ($\Delta T = 0$) in Fig. A2.20 leads to,

$$E_{app} = \mu^{1/(\mu-1)} RT_m^2 C_{p,m}^{ex}/\Delta H. \quad \text{(A2.22)}$$

Given that $\lim_{\mu\to 1} \mu^{1/(\mu-1)} = e$, the equation corresponding to the two-state irreversible model with first-order kinetics is:

$$E_{app} = e\, RT_m^2 C_{p,m}^{ex}/\Delta H, \quad \text{(A2.23)}$$

which was obtained by Sanchez-Ruiz et al. (1988a) using a different procedure (Eq. (A2.23) can also be arrived at by setting $\Delta T = 0$ in Eq. A2.21.

This research was supported by grants PB87-0871 from the Direccion General de Investigacion Cientifica y Tecnica and 0460.E from the Biotechnology Action Programme of the European Communities.

Received for publication 20 December 1990 and in final form 6 November 1991.

REFERENCES

Bertazzon, A., G. H. Tian, A. Lamblin, and T.Y. Tsong. 1990. Enthalpic and entropic contributions to actin stability: calorimetry,

[5]Eq. A2.20 must be applied within the temperature range $0 \le T \le T'$, where T' is equal to $T_m + (RT_m^2/E_{app})\ln(\mu/(\mu - 1))$; note that, for $T = T'$, $C_p^{ex} = 0$, and that, for $T > T'$, it is not possible to calculate C_p^{ex} values, as the last bracket in Eq. A2.20 yields a negative number (for fitting purposes, C_p^{ex} has been set equal to zero for any temperature above T'). This is a consequence of the fact that Eq. A2.1 is an approximation based on the assumption that $C_U \ll C_N$ (situation C); obviously, this assumption will break down at a given temperature during the scan given that, as the temperature increases, the concentration of native plus unfolded protein becomes lower and the preliminary equilibrium is displaced towards the monomeric unfolded species. Thus, a DSC transition will be described by models IV or VI in situation C, if essentially all the protein is already in the final state at the temperatures in which Eq. A2.1 (and, hence, Eq. A2.20) no longer holds true.

circular dichroism, and fluorescence study and effects of calcium. *Biochemistry.* 29:291–298.

Brandts, J. F., C. Q. Hu, L.-N. Lin, and M. T. Mas. 1989. A simple model for proteins with interacting domains. Applications to scanning calorimetry data. *Biochemistry.* 28:8588–8596.

Conejero-Lara, F., P. L. Mateo, F. X. Aviles, and J. M. Sanchez-Ruiz. 1991. The effect of Zn^{2+} on the thermal denaturation of carboxypeptidase B. *Biochemistry.* 30:2067–2072.

Edge, V., N. M. Allewell, and J. M. Sturtevant. 1985. High-resolution differential scanning calorimetric analysis of the subunits of *Escherichia coli* aspartate transcarbamoylase. *Biochemistry.* 24:5899–5906.

Freire, E., and R. L. Biltonen. 1978. Statistical mechanical deconvolution of thermal transitions in macromolecules. I. Theory and applications to homogeneous systems. *Biopolymers.* 17:463–479.

Freire, E., W. W. van Osdol, O. L. Mayorga, and J. M. Sanchez-Ruiz. 1990. Calorimetrically determined dynamics of complex unfolding transitions in proteins. *Annu. Rev. Biophys. Biophys. Chem.* 19:159–188.

Fukada, H., J. M. Sturtevant, and F. A. Quiocho. 1983. Thermodynamics of the binding of L-arabinose and of D-galactose to the L-arabinose-binding protein of *Escherichia coli. J. Biol. Chem.* 258:13193–13198.

Galisteo, M. L., P. L. Mateo, and J. M. Sanchez-Ruiz. 1991. A kinetic study on the irreversible thermal denaturation of yeast phosphoglycerate kinase. *Biochemistry.* 30:2061–2066.

Goins, B., and E. Freire. 1988. Thermal stability and intersubunit interactions of cholera toxin in solution and in association with its cell-surface receptor ganglioside G_{M1}. *Biochemistry.* 27:2046–2052.

Guzman-Casado, M., A. Parody-Morreale, P. L. Mateo, and J. M. Sanchez-Ruiz. 1990. Differential scanning calorimetry of lobster haemocyanin. *Eur J. Biochem.* 188:181–185.

Hu, C. Q., and J. M. Sturtevant. 1987. Thermodynamic study of yeast phosphoglycerate kinase. *Biochemistry.* 26:178–182.

Hu, C. Q., and J. M. Sturtevant. 1989. A differential scanning calorimetric study on the binding of sulfate ion and of Cibacron blue F3GA to yeast phosphoglycerate kinase. *Biochemistry.* 28:813–818.

Jencks, W. P. 1987. Catalysis in Chemistry and Enzymology. Dover Publications Inc., New York. 836 pp.

Klibanov, A. M., and T. J. Ahern. 1987. Thermal stability of proteins. *In* Protein Engineering. D. L. Oxender and C. F. Fox, editors. Alan R. Liss, New York. 213—218.

Lepock, J. R., A. M. Rodahl, C. Zhang, M. L. Heynen, B. Waters, and K.-H. Cheng. 1990. Thermal denaturation of the Ca^{2+}-ATPase of sarcoplasmic reticulum reveals two thermodynamically independent domains. *Biochemistry.* 29:681–689.

Lowry, T. H., and K. S. Richardson. 1976. Mechanism and theory in organic chemistry. Harper and Row, New York. 748 pp.

Lumry, R., and H. Eyring. 1954. Conformation changes of proteins. *J. Phys. Chem.* 58:110–120.

Manly, S. P., K. S. Matthews, and J. M. Sturtevant. 1985. Thermal denaturation of the core protein of *lac* repressor. *Biochemistry.* 24:3842–3846.

Morin, P. E., D. Diggs, and E. Freire. 1990. Thermal stability of membrane-reconstituted yeast cytochrome c oxidase. *Biochemistry.* 29:781–788.

Privalov, P. L. 1979. Stability of proteins. Small globular proteins. *Adv. Protein Chem.* 33:167–241.

Privalov, P. L. 1982. Stability of proteins. Proteins which do not present a single cooperative system. *Adv. Protein Chem.* 35:1–104.

Privalov, P. L. 1989. Thermodynamic problems of protein structure. *Annu. Rev. Biophys. Biophys. Chem.* 18:47–69.

Privalov, P. L., and L. V. Medved'. 1982. Domains in the fibrinogen molecule. *J. Mol. Biol.* 159:665–683.

Ramsay, G., and E. Freire. 1990. Linked thermal and solute perturbation analysis of cooperative domain interactions in proteins. Structural stability of diphtheria toxin. *Biochemistry.* 29:8677–8683.

Sanchez-Ruiz, J. M., J. L. Lopez-Lacomba, M. Cortijo, and P. L. Mateo. 1988a. Differential scanning calorimetry of the irreversible thermal denaturation of thermolysin. *Biochemistry.* 27:1648–1652.

Sanchez-Ruiz, J. M., J. L. Lopez-Lacomba, P. L. Mateo, M. Vilanova, M. A. Serra, and F. X. Aviles. 1988b. Analysis of the thermal unfolding of procine procarboxypeptidase A and its functional pieces by differential scanning calorimetry. *Eur. J. Biochem.* 176:225–230.

Sturtevant, J. M. 1987. Biochemical applications of differential scanning calorimetry. *Annu. Rev. Phys. Chem.* 38:463–488.

Takahashi, K., and J. M. Sturtevant. 1981. Thermal denaturation of *Streptomyces* subtilisin inhibitor, subtilisin BPN', and the inhibitor-subtilisin complex. *Biochemistry.* 20:6185–6190.